

rials values of  $K_{uQDSL/Au} = K_{QDSL} + K_{Au}$ ,  $K_{u(Bi,Sb)_2(Se,Te)_3/Au} = K_{(Bi,Sb)_2(Se,Te)_3} + K_{Au}$ ,  $R_{uQDSL/Au} = R_{QDSL} + R_{Au}$ , and  $R_{u(Bi,Sb)_2(Se,Te)_3/Au} = R_{(Bi,Sb)_2(Se,Te)_3} + R_{Au}$  from the measured thermoelectric properties of the individual thermoelements and their dimensions for the two devices as 0.00044 W/K, 0.00061 W/K, 0.094  $\Omega$ , and 0.074  $\Omega$ , respectively. The calculated  $K_u$ 's and  $R_u$ 's are first-order estimates of the actual values, and many factors may change their values, such as the quality of the plating and soldering techniques used to form electrical contacts.

**Conclusions.** TE cooling test devices have been made from PbSeTe/PbTe QDSL material. 43.7 K of cooling below room temperature was measured, even though one leg was a zero ZT gold wire. This compares to 30.8 K of cooling for the conventional (Bi,Sb)<sub>2</sub>(Se,Te)<sub>3</sub> material in the same test setup and the same hot junction temperature and about the same aspect ratio. We believe a TE material has been found that is a better room temperature cooler material than bulk (Bi,Sb)<sub>2</sub>(Se,Te)<sub>3</sub> solid solution alloy material. Device measurements indicate the attainment of device  $Z_4T$  and a materials or intrinsic ZT in the range of 1.3 to 1.6 at room temperature. The enhanced TE device performance at 300 K of the PbSeTe/PbTe QDSL material is believed to be (at this point in time) almost entirely due to a high density of quantum nanodots with essentially 100% PbSe composition embedded in a three-dimensional slab matrix of PbTe. As described in the SOM, the first quaternary PbSnSeTe QDSL TE materials have been grown by MBE and have conservatively estimated intrinsic ZT values of 2.0 at 300 K. Further improvements are anticipated, as both the materials and devices are not optimized.

#### References and Notes

1. T. C. Harman, P. J. Taylor, D. L. Spears, M. P. Walsh, *J. Electron. Mater.* **29**, L1 (2000).
2. \_\_\_\_\_, in *18th International Conference on Thermoelectrics: ICT Symposium Proceedings*, Baltimore, MD (IEEE, Piscataway, NJ, 1999), pp. 280–284.
3. M. S. Dresselhaus, in *Recent Trends in Thermoelectric Materials Research III, Semiconductors and Semimetals*, T. W. Tritt, vol. Ed. R. K. Willardson, E. R. Weber, series Eds. (Academic Press, London, 2001), vol. 71, chap. 1. See also the other four chapters in vol. 71, as well as vols. 69 and 70.
4. R. M. Rowe, Ed., *CRC Handbook of Thermoelectrics* (CRC Press, Boca Raton, FL, 1995).
5. T. C. Harman, J. M. Honig, *Thermoelectric and Thermomagnetic Effects and Applications* (McGraw-Hill, New York, 1967), p. 291.
6. R. Venkatasubramanian, E. Sivola, T. Colpitts, B. O'Quinn, *Nature* **413**, 597 (2001).
7. W. M. Yim, F. D. Rosi, *Solid-State Electron.* **15**, 1121 (1972).
8. P. J. Taylor, thesis, Univ. of Virginia (1993).
9. T. C. Harman, *J. Appl. Phys.* **29**, 1373 (1958).
10. \_\_\_\_\_, J. H. Cahn, M. J. Logan, *J. Appl. Phys.* **30**, 1351 (1959).
11. G. S. Nolas, J. Sharp, H. J. Goldsmid, *Thermoelectrics* (Springer-Verlag, Berlin, 2001), p. 100.

12. W. L. Liu, T. Borca-Tasciuc, G. Chen, J. L. Liu, K. L. Wang, *J. Nanosci. Nanotechnol.* **1**, 39 (2001).
13. Sponsored by the Department of the Navy and the Defense Advanced Research Projects Agency (DARPA) under Air Force contract no. F19628-00-C-0002. The opinions, interpretations, conclusions, and recommendations are those of the authors and are not necessarily endorsed by the Department of Defense.

**Supporting Online Material**  
www.sciencemag.org/cgi/content/full/11/29/5590/2229/DC1  
SOM Text  
References and Notes  
Fig. S1  
Tables S1, S2, S3

15 April 2002; accepted 28 August 2002

## Establishment and Maintenance of a Heterochromatin Domain

Ira M. Hall,<sup>1,2\*</sup> Gurumurthy D. Shankaranarayana,<sup>1\*</sup>  
Ken-ichi Noma,<sup>1\*</sup> Nabieh Ayoub,<sup>3</sup> Amikam Cohen,<sup>3</sup>  
Shiv I. S. Grewal<sup>1,2†</sup>

The higher-order assembly of chromatin imposes structural organization on the genetic information of eukaryotes and is thought to be largely determined by posttranslational modification of histone tails. Here, we study a 20-kilobase silent domain at the mating-type region of fission yeast as a model for heterochromatin formation. We find that, although histone H3 methylated at lysine 9 (H3 Lys<sup>9</sup>) directly recruits heterochromatin protein Swi6/HP1, the critical determinant for H3 Lys<sup>9</sup> methylation to spread in cis and to be inherited through mitosis and meiosis is Swi6 itself. We demonstrate that a centromere-homologous repeat (*cenH*) present at the silent mating-type region is sufficient for heterochromatin formation at an ectopic site, and that its repressive capacity is mediated by components of the RNA interference (RNAi) machinery. Moreover, *cenH* and the RNAi machinery cooperate to nucleate heterochromatin assembly at the endogenous *mat* locus but are dispensable for its subsequent inheritance. This work defines sequential requirements for the initiation and propagation of regional heterochromatic domains.

In eukaryotes, the organization of chromatin into higher-order structures governs diverse chromosomal processes. Besides creating distinct metastable transcriptional domains during cellular differentiation, the formation of higher-order chromatin domains is widely recognized to be essential for imprinting, dosage compensation, recombination, and chromosome condensation (1–4). The assembly of heterochromatin at centromeres is essential for the accurate segregation of chromosomes during cell division, and the formation of such specialized structures at telomeres protects chromosomes from degradation and from aberrant chromosomal fusions (2). Moreover, repetitive DNA sequences such as transposable elements are often assembled into heterochromatin that, in addition to its role in transcriptional repression, maintains genome integrity by suppressing recombination between repetitive elements (5).

The posttranslational modification of his-

tone tails plays a causal role in the assembly of higher-order chromatin, and accumulating evidence suggests that patterns of histone modification specify discrete downstream regulatory events (6, 7). The factors that define particular chromosomal domains as preferred sites of heterochromatin assembly are largely uncharacterized. It has been suggested that heterochromatin protein complexes are preferentially targeted to repetitive DNA elements, such as commonly found at the pericentric heterochromatin and intergenic regions of higher eukaryotes (8, 9). Interestingly, rather than any specific sequence motif, the repetitive nature of transgene arrays alone appears to be sufficient for heterochromatin formation (9, 10). Furthermore, studies of position effect variegation have shown that heterochromatin complexes possess the ability to spread along the chromosomes, resulting in the heritable inactivation of nearby sequences (2).

Higher-order chromatin structure is critical for the functional organization of centromeres and the mating-type region of the fission yeast *Schizosaccharomyces pombe* (2). At centromeres, tandem and inverted arrays of the *dg* and *dh* centromeric repeats surrounding the unique central core are assembled into heterochromatin and are bound by CENP-B proteins that resemble the trans-

<sup>1</sup>Cold Spring Harbor Laboratory, <sup>2</sup>Watson School of Biological Sciences, Post Office Box 100, Cold Spring Harbor, NY 11724, USA. <sup>3</sup>Department of Molecular Biology, The Hebrew University-Hadassah Medical School, Jerusalem, Israel 91010.

\*These authors contributed equally to this work.

†To whom correspondence should be addressed. E-mail: grewal@cshl.org

posase encoded by POGO-like elements (11–14). At the mating-type region, a 20-kb domain containing the *mat2* and *mat3* silent donor loci and the interval between them, known as the *K*-region, are subject to heterochromatin-mediated silencing and recombinational suppression (2). Heterochromatin formation at the centromeres and within the silent mating-type (*mat2/3*) interval requires many of the same trans-acting factors, including histone deacetylases (HDACs); the H3 Lys<sup>9</sup>-specific methyltransferase Clr4; and Swi6, the fission yeast counterpart to mammalian HP1 (13, 15–18).

We previously showed that formation of heterochromatin within the entire 20 kb of the silent mating-type region depends on H3 Lys<sup>9</sup> methylation by Clr4 and the subsequent binding of Swi6, both of which are restricted to this domain by the IR-R and IR-L boundary elements (19). The *K*-region, in particular the 4.3-kb *cenH* sequence that contains several clusters of short direct repeats and shares strong homology with *dg* and *dh* centromeric elements, is important for heterochromatin assembly (20). Replacement of the *cenH*-containing region with *ura4*<sup>+</sup> (*KΔ::ura4*<sup>+</sup>) results in a metastable locus that displays alternative silenced (*ura4-off*) and expressed (*ura4-on*) epigenetic states (21, 22). This variegation of *ura4*<sup>+</sup> expression is due to defects in establishment of the silenced chromatin state in *KΔ::ura4*<sup>+</sup> cells. Once assembled, the *ura4-off* state is remarkably stable during both mitosis and meiosis. Moreover, maintenance of the *ura4-off* state

requires functional Swi6, Clr4, and HDACs.

**Maintenance of H3 Lys<sup>9</sup> methylation depends on Swi6.** Our previous findings predicted a model for heterochromatin formation in which the cooperative activity of HDACs and the H3 Lys<sup>9</sup> methyltransferase Clr4 establish a “histone code” that is essential for localization of Swi6 to silenced genomic locations (18). Although H3 Lys<sup>9</sup> methylation is required for the chromatin association of Swi6, mutations in Swi6 had minimal effects on levels of H3 Lys<sup>9</sup> methylation at the *Kint2::ura4*<sup>+</sup> reporter gene located within the *cenH* repeat, indicating that H3 Lys<sup>9</sup> methylation acts upstream of Swi6 (18) (Fig. 1A). However, we discovered that, in *KΔ::ura4*<sup>+</sup> cells lacking the *cenH* repeat, the presence of H3 Lys<sup>9</sup> methylation strictly depends on Swi6, as shown by chromatin immunoprecipitation (ChIP) experiments (Fig. 1B). This indicates that a portion of the sequence deleted in the *KΔ::ura4*<sup>+</sup> strain has the ability to recruit H3 Lys<sup>9</sup> methylation by itself and that flanking sequences present in the *KΔ::ura4*<sup>+</sup> strain are capable of recruiting and maintaining H3 Lys<sup>9</sup> methylation only in the presence of Swi6.

The *KΔ::ura4*<sup>+</sup> *ura4-off* cells exhibit considerably higher levels of Swi6 throughout their *mat2/3* region than *ura4-on* cells (21). Consistent with these findings, we observed higher levels of H3 Lys<sup>9</sup> methylation at the mating-type region in *ura4-off* cells (Fig. 1C). Additional copies of *swi6*<sup>+</sup> resulted in increases in H3 Lys<sup>9</sup> methylation and Swi6 levels at the *mat2/3* region, further supporting

the possibility that Swi6 promotes H3 Lys<sup>9</sup> methylation at the *mat* locus (Fig. 1D). The increase in levels of Swi6 and H3 Lys<sup>9</sup> methylation also correlates with an increase in *ura4-on* to *ura4-off* conversion. Interestingly, multiple copies of *clr4*<sup>+</sup> do not cause considerable changes in H3 Lys<sup>9</sup> methylation and Swi6 localization. These results underscore the importance of Swi6 in the maintenance of H3 Lys<sup>9</sup> methylation and heterochromatin in the absence of the *cenH* repeat and are consistent with our previous work suggesting that Swi6 protein is a critical component of the epigenetic imprint (21).

The interdependence of Swi6 and H3 Lys<sup>9</sup> methylation at the *mat2/3* region suggests an “epigenetic loop” for inheritance of the heterochromatic state, whereby H3 Lys<sup>9</sup> methylation and Swi6 mutually support their own maintenance in a self-perpetuating manner. This mechanism would predict that differential localization of Swi6 and H3 Lys<sup>9</sup> methylation patterns defining *ura4-on* and *ura4-off* epialleles would be inherited in cis and maintained even when these epialleles are combined into the same environment of a diploid nucleus. To test this possibility, we crossed *ura4-off* and *ura4-on* strains differing at the *his2* marker tightly linked to the *mat* locus (*ura4-off his2*<sup>-</sup>; *ura4-on his2*<sup>+</sup>). Sporulation and tetrad analysis of the resulting diploid showed a 2 Ura<sup>+</sup> His<sup>+</sup>: 2 Ura<sup>-</sup> His<sup>-</sup> segregation pattern in each tetrad, indicating that the epigenetic state of the *mat* region is inherited in cis and segregates as

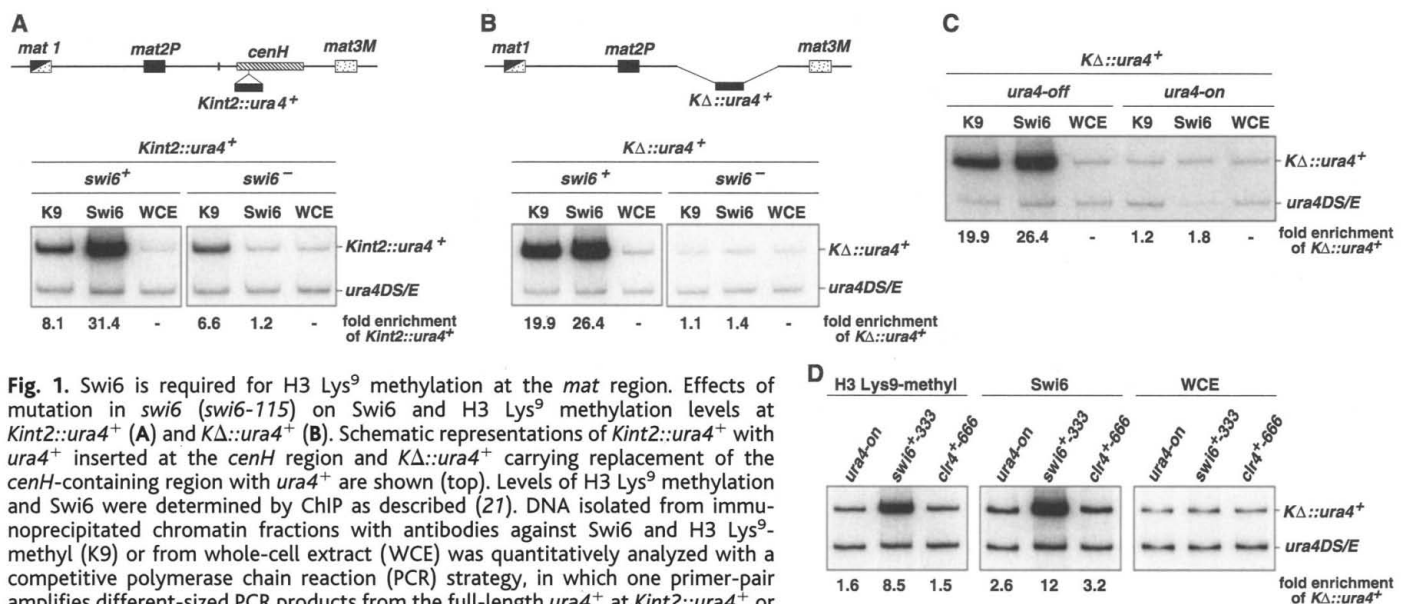


**Fig. 1.** Swi6 is required for H3 Lys<sup>9</sup> methylation at the *mat* region. Effects of mutation in *swi6* (*swi6-115*) on Swi6 and H3 Lys<sup>9</sup> methylation levels at *Kint2::ura4*<sup>+</sup> (A) and *KΔ::ura4*<sup>+</sup> (B). Schematic representations of *Kint2::ura4*<sup>+</sup> with *ura4*<sup>+</sup> inserted at the *cenH* region and *KΔ::ura4*<sup>+</sup> carrying replacement of the *cenH*-containing region with *ura4*<sup>+</sup> are shown (top). Levels of H3 Lys<sup>9</sup> methylation and Swi6 were determined by ChIP as described (21). DNA isolated from immunoprecipitated chromatin fractions with antibodies against Swi6 and H3 Lys<sup>9</sup>-methyl (K9) or from whole-cell extract (WCE) was quantitatively analyzed with a competitive polymerase chain reaction (PCR) strategy, in which one primer-pair amplifies different-sized PCR products from the full-length *ura4*<sup>+</sup> at *Kint2::ura4*<sup>+</sup> or *KΔ::ura4*<sup>+</sup> locations and the control *ura4DS/E* minigene at the endogenous location. PCR fragments were resolved on polyacrylamide gels and quantified with a PhosphorImager. The ratios of *ura4*<sup>+</sup> and *ura4DS/E* signals in the ChIP and WCE lanes were used to calculate the relative precipitated fold enrichment, shown below each lane. (C) Swi6 and H3 Lys<sup>9</sup> methylation (K9) are differentially localized in the *ura4-off* and *ura4-on* epialleles. ChIP was performed on *KΔ::ura4*<sup>+</sup> cells differing only in the epigenetic state of their *mat* locus. (D) Multiple copies of *swi6*<sup>+</sup> cause an increase in H3 Lys<sup>9</sup> methylation levels at *KΔ::ura4*<sup>+</sup>. Three copies of *swi6*<sup>+</sup> (*swi6*<sup>+</sup>-333) or six copies of *clr4*<sup>+</sup> (*clr4*<sup>+</sup>-666) inserted at their endogenous chromosomal location were combined with the *ura4-on* epiallele through genetic crosses. The quantitative measurement of Swi6 and H3 Lys<sup>9</sup> methylation (K9) levels was carried out with ChIP.

a marker linked to the respective *his2* alleles (Fig. 2) (22). Consistent with the ability of heterochromatin complexes to maintain themselves, ChIP analysis showed that the different levels of H3 Lys<sup>9</sup> methylation and Swi6 localization corresponding to the *ura4-on* and *ura4-off* states are inherited in cis and are stable through meiosis (Fig. 2).

***cenH* is a nucleation center.** Genetic studies with the *KΔ::ura4<sup>+</sup>* reporter highlighted the requirement of *cenH* in efficient establishment of the silenced chromatin state at the *mat* region (20). Furthermore, the persistence of H3 Lys<sup>9</sup> methylation at *Kint2::ura4<sup>+</sup>* in *swi6* mutant cells (see Fig. 1A) led us to hypothesize that heterochromatin formation is initiated at the *cenH* repeat but requires Swi6 to spread across the entire silenced domain. This hypothesis predicts that H3 Lys<sup>9</sup> methylation will be restricted to *cenH* in the absence of Swi6. To test this, we performed high-resolution ChIP analysis of H3 Lys<sup>9</sup> methylation and H3 Lys<sup>4</sup> methylation [a modification associated with active chromatin (19)] at the *mat* region in wild-type and *swi6* mutant strains (Fig. 3). We found that H3 Lys<sup>9</sup> methylation in the *swi6* mutant strain was restricted to a small portion of the *mat* region encompassing *cenH*. The loss of H3 Lys<sup>9</sup> methylation at the *mat2/3* interval was correlated with only a slight increase in H3 Lys<sup>4</sup> methylation, although we did observe a small peak directly at the transcribed portion of

*cenH* (Fig. 3) (23). These data indicate that the recruitment of H3 Lys<sup>9</sup> methylation to the *cenH* repeat region occurs via a Swi6-independent mechanism and suggest that Swi6 is required for the spreading and maintenance of H3 Lys<sup>9</sup> methylation across the rest of the silent *mat2/3* interval.

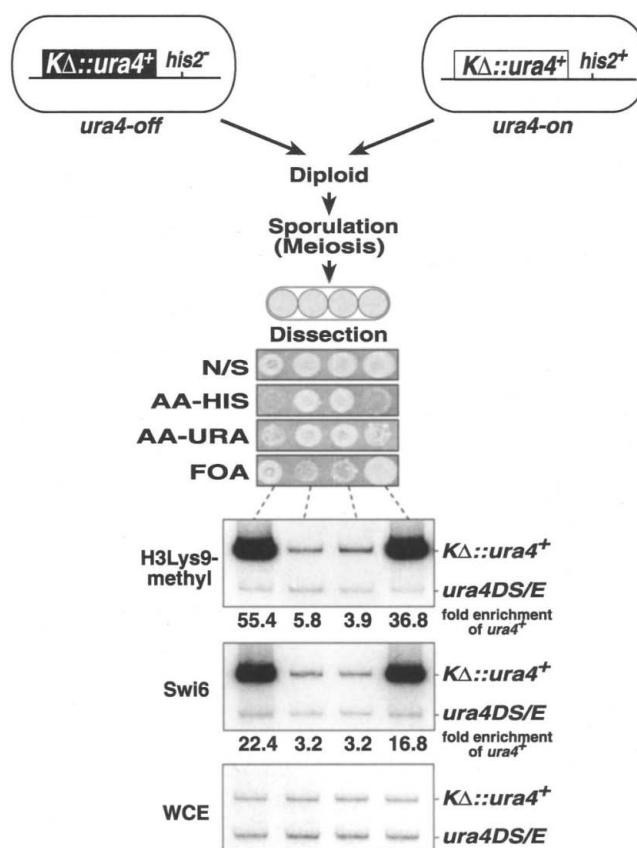
The results presented above suggest that *cenH* directly participates in heterochromatin formation by promoting recruitment of histone-modifying enzymes and Swi6. To test this, we examined the contribution of *cenH* to heterochromatin formation at an ectopic, otherwise euchromatic site. We used a strain in which the 3.6-kb *cenH* repeat fused to an *ade6<sup>+</sup>* reporter gene (*cenH-ade6<sup>+</sup>*) was inserted into the *ura4* gene. In wild-type cells, *cenH* confers repression on the reporter gene and results in a variegated expression phenotype (Fig. 4A) (24). Silencing at the ectopic site depends on functional Ctr4 and Swi6 and correlates with preferential enrichment of both H3 Lys<sup>9</sup> methylation and Swi6 (Fig. 4B). Similar to the *mat* region, H3 Lys<sup>9</sup> methylation at the ectopic *cenH-ade6<sup>+</sup>* location occurs independently of Swi6. These data demonstrate that the *cenH* repeat is sufficient to induce heterochromatin formation and that it requires similar chromatin modification and trans-acting factors as the endogenous *mat* region.

***cenH*-mediated silencing requires the RNAi machinery.** RNA interference (RNAi) is a mechanism through which double-stranded RNA (dsRNA) silences cognate genes (25). The dsRNA serves as a sequence-specific trigger for destruction of homologous RNAs and has been shown in some cases to result in the epigenetic silencing of homologous genes (26, 27). *S. pombe* contains homologs of the Argonaute (*ago1*), Dicer (*dcr1*), and RNA-dependent RNA polymerase (*rdp1*) genes required for RNAi-related processes in other systems (25, 28, 29). Our recent analysis showed silencing and heterochromatin assembly at centromeric repeats in fission yeast require these factors (30). Interestingly, we found that deletions of *ago1*, *dcr1*, or *rdp1* abolished repression of the *cenH-ade6<sup>+</sup>* reporter (Fig. 4A). Furthermore, ChIP analysis revealed that the locus was no longer able to recruit and/or maintain H3 Lys<sup>9</sup> methylation and Swi6 (Fig. 4B). These data indicate that *cenH*-induced silencing and the corresponding H3 Lys<sup>9</sup> methylation and Swi6 localization to the ectopic domain require the RNAi machinery.

**RNAi machinery is required for initiation of heterochromatin.** To investigate the role of the RNAi machinery in heterochromatin assembly at the endogenous *mat* region, we introduced the *Kint2::ura4<sup>+</sup>* reporter into the respective mutant backgrounds with genetic crosses. Surprisingly, silencing at the *mat* locus was intact in the mutant strains (Fig. 5A), and the efficiency of mating-type interconversion, which depends on the heterochromatic structure at the *mat2/3* region, was unaffected. More importantly, the levels of Swi6 protein and H3 Lys<sup>9</sup> methylation at the *mat2/3* region were comparable in wild-type and mutant strains. These analyses suggest that the RNAi machinery is dispensable for maintaining a preassembled heterochromatic state.

We next addressed the role of RNAi components in the establishment of silencing by examining their involvement in the initiation step of heterochromatin formation. The deacetylase inhibitor trichostatin A (TSA) has previously been shown to erase the epigenetic imprint governing silencing at the *mat* region (17). We observed that treatment of wild-type and mutant cells with TSA for 10 generations alleviated *Kint2::ura4<sup>+</sup>* silencing in most cells. After an additional 10 generations of growth in the absence of TSA, wild-type cells fully reestablished silencing at the *mat2/3* locus (Fig. 5B). In striking contrast, *ago1Δ*, *dcr1Δ*, and *rdp1Δ* strains were defective in the establishment of heterochromatin at the *mat2/3* locus because only a relatively small proportion of cells acquired silencing of *Kint2::ura4<sup>+</sup>* (Fig. 5B). ChIP analysis demonstrated that, after recovery from TSA treatment, the levels of H3 Lys<sup>9</sup> methylation and Swi6 were considerably higher at the *mat* region of wild-type cells

**Fig. 2.** Differential H3 Lys<sup>9</sup> methylation and Swi6 localization patterns shown by *ura4-off* and *ura4-on* epialleles are stably inherited in cis. Diagram of the cross is shown (top). *KΔ::ura4<sup>+</sup>* strains carrying *ura4-off* (*his2<sup>-</sup>*) and *ura4-on* (*his2<sup>+</sup>*) epialleles differing at the tightly linked *his2* marker were crossed, allowed at least 30 generations of diploid growth, sporulated, and subjected to tetrad analysis. Resulting colonies were replicated onto nonselective medium (N/S), medium lacking uracil (AA-URA), medium lacking histidine (AA-HIS), or medium containing 5-fluoroorotic acid (FOA), which selects for the growth of *Ura<sup>-</sup>* cells. Segregants from individual tetrads were subjected to ChIP analysis with Swi6 and H3 Lys<sup>9</sup>-methyl antibodies (bottom).



compared with RNAi mutant cells (Fig. 5B). This indicates that the RNAi deletion strains are unable to efficiently establish the heterochromatic state after it has been erased.

To genetically test the role of RNAi machinery in the initiation of heterochromatin formation, we used a *clr4Δ* strain carrying the *Kint2::ura4<sup>+</sup>* reporter gene to construct diploid strains heterozygous for *clr4Δ* and homozygous for *ago1Δ*, *dcr1Δ*, or *rdp1Δ* (for example, *clr4<sup>+</sup>/clr4Δ dcr1Δ/dcr1Δ*). Because Clr4 is the sole H3 Lys<sup>9</sup>-specific methyltransferase in fission yeast, the *mat* locus propagated in a *clr4Δ* background is completely devoid of H3 Lys<sup>9</sup> methylation and Swi6 protein (18). Diploids were sporulated to obtain *ago1Δ clr4<sup>+</sup>*, *dcr1Δ clr4<sup>+</sup>*, or *rdp1Δ clr4<sup>+</sup>* haploid segregants. Phenotypic analysis of the segregants that contain a functional H3 Lys<sup>9</sup> methyltransferase but lack RNAi machinery revealed severe defects in heterochromatin assembly at the *mat* locus, as observed by both *Kint2::ura4<sup>+</sup>* expression and the decreased efficiency of mating-type interconversion (Fig. 5C). ChIP analysis showed that the RNAi mutant strains containing a *mat* region derived from the *clr4Δ* background have less H3 Lys<sup>9</sup> methylation and Swi6 protein than strains in which the *mat* region was derived from a wild-type background (Fig. 5C). It is noteworthy, however, that after introduction of the *clr4<sup>+</sup>* allele the proportion of cells with a silenced *mat* region increases each generation in an inefficient and highly stochastic manner, indicating that heterochromatin formation eventually does occur in the absence of the RNAi machinery, likely via an alternative Swi6-based mechanism.

These data indicate that, although the RNAi mutant strains are able to maintain a silenced *mat* region when it is derived from a wild-type parent, they are unable to effectively establish silencing at a *mat* region rendered epigenetically active by TSA treatment or propagation in a *clr4Δ* background. These findings are consistent with the inefficient establishment of silencing observed in *KΔ::ura4<sup>+</sup>* cells carrying deletion of *cenH* (20) and further suggest that the RNAi machinery and *cenH* repeat operate in the same pathway to establish heterochromatin.

**A model for heterochromatin assembly.** The results presented here define sequential events in the assembly of heterochromatin at the mating-type region of fission yeast. We show that the establishment of epigenetic silencing requires an initial nucleation event and is distinct in this respect from mechanisms that act in cis to reinforce propagation of the heterochromatic state. Supporting our identification of *cenH* as an RNAi-dependent heterochromatin nucleation center, a portion of *cenH* homologous to the *dh* repeat is the minimal sequence sufficient for silencing at an ectopic site (24). This sequence is located within the transcribed region of *cenH* (23) and is homologous to some

of the recently described heterochromatic siRNAs (31). In our current model, transcripts derived from *cenH* are processed by the RNAi machinery, and resulting RNA intermediates directly recruit HDAC and H3 Lys<sup>9</sup> methyltransferase activities to the *mat* locus. This may occur through an interaction between siRNA and the chromodomain (32) of Clr4 and/or the WD-40 repeat containing protein Rik1, also required for H3 Lys<sup>9</sup> methylation (18). This initial recruitment is proposed to nucleate heterochromatin by creating H3 Lys<sup>9</sup> methylated binding sites for Swi6 (33). Once bound to chromatin, Swi6 serves as a platform for the recruitment of histone-modifying activities that create additional Swi6 binding sites on adjacent nucleosomes, thus enabling spreading to occur in a stepwise manner (2, 21). The presence of chromatin boundaries ensures that heterochromatin does not spread to neighboring euchro-

matic regions (19). Upon chromosome replication, parental histone H3 (34) and Swi6 are hypothesized to segregate randomly to the daughter chromatids, and Swi6-based activities serve to imprint the parental histone modification pattern onto newly assembled nucleosomes by the same mechanism with which they promote spreading in cis. Because heterochromatin formation eventually occurs without the RNAi machinery, and because stochastic initiation events also occur in the absence of *cenH*, we predict the existence of additional Swi6-dependent, RNAi-independent nucleation sites in the *mat* region.

The mechanism proposed above is reminiscent of mammalian X-chromosome inactivation, in which an H3 Lys<sup>9</sup> methylation hotspot upstream of the Xist locus serves to initiate the cooperative spreading of Xist noncoding RNA and H3 Lys<sup>9</sup> methylation across the entire in-

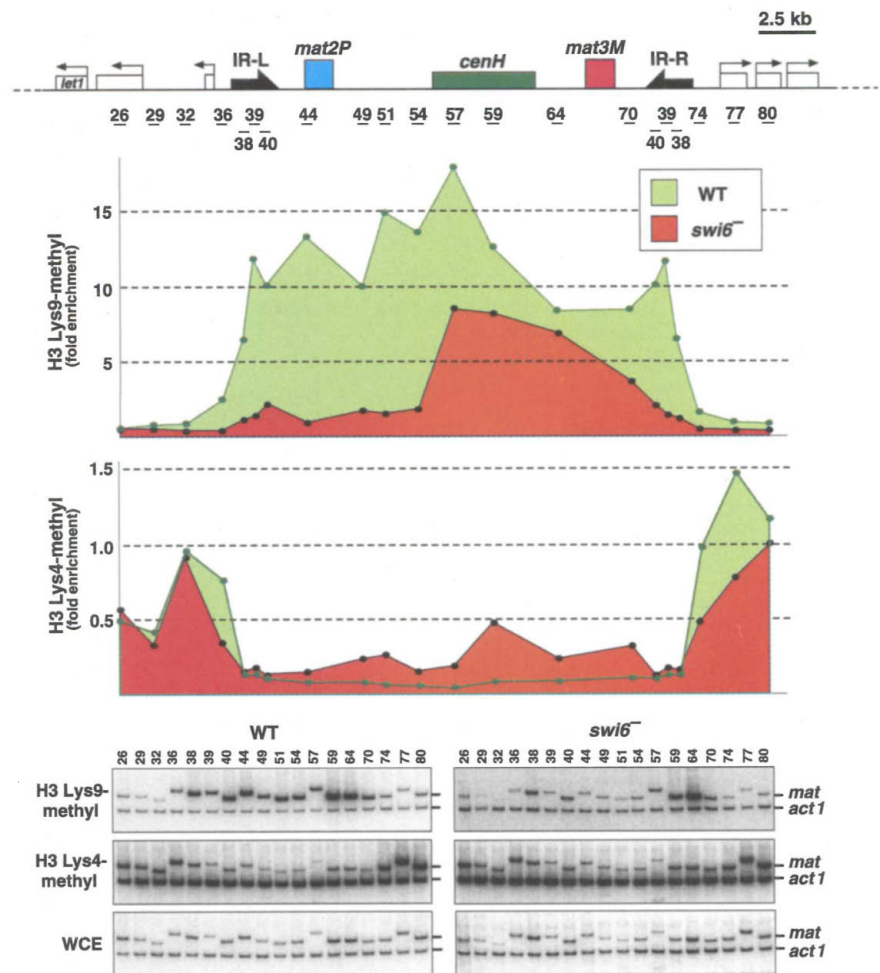


**Fig. 3.** Effects of mutation in *swi6* on H3 Lys<sup>9</sup> and H3 Lys<sup>4</sup> methylation at the *mat2/3* interval. A physical map of the silent mating-type region is shown (top). High-resolution mapping of H3 Lys<sup>9</sup> or H3 Lys<sup>4</sup> methylation was carried out as described (19). ChIP with antibodies to methylated H3 Lys<sup>9</sup> or H3 Lys<sup>4</sup> was used to measure H3 methylation levels at respective sites throughout the *mat2/3* interval. DNA isolated from ChIP and WCE fractions was subjected to multiplex PCR to amplify DNA fragments from the *mat* locus as well as an *act1* fragment serving as an internal amplification control. The ratios of the *mat* locus and control *act1* signals present in WCE were used to calculate relative fold enrichment of precipitated samples. Quantitation of these results is plotted in alignment with a map of the *mat* locus. WT, wild type.

active X (35). Significantly, once silencing is established, Xist RNA becomes dispensable and the heterochromatic state persists in the absence of the initial stimulus (3). Mechanisms involving RNAi-like processes may also operate in the lineage-specific establishment of silenced chromatin domains during development.

It is remarkable that, in fission yeast, the

mating-type locus appears to have used a repetitive DNA element to organize a highly specialized chromatin structure that controls transcriptional silencing, recombinational suppression, and the nonrandom utilization of silent cassettes during mating-type switching. Similar processes may influence a variety of chromosomal func-

tions important for preserving genomic integrity, such as prohibition of wasteful transcription and suppression of deleterious recombination between repetitive elements. In this regard, it should be noted that the presence of large, repetitive heterochromatic regions is widespread among eukaryotes, and, in *Drosophila*, plants, mammals, and some fungi, the introduction of repetitive sequences of diverse origin can stimulate pathways leading to heterochromatin formation (8, 9, 36, 37). Future analysis of the connection between RNAi and chromatin assembly will provide insight into the epigenetic organization of eukaryotic genomes.

**Fig. 4.** *cenH*-mediated heterochromatin formation at an ectopic site requires RNAi machinery. (A) Deletions of the components of RNAi machinery suppress variegation of *cenH-ade6<sup>+</sup>* expression. Schematic representation of the *cenH-ade6<sup>+</sup>* construct inserted into the *ura4* locus is shown (top). Strains carrying *cenH-ade6<sup>+</sup>* in *ago1Δ*, *dcr1Δ*, or *rdp1Δ* deletion background were constructed by genetic crosses. The *cenH-ade6<sup>+</sup>* expression phenotypes were scored by a colony color assay. Cells were plated on adenine-limiting yeast extract medium and incubated at 33°C for 3 days before photography. The red or white color of colonies implies *Ade<sup>-</sup>* or *Ade<sup>+</sup>* phenotype, respectively. Wild-type cells display 21% red, 11% pink, and 68% white colonies, whereas mutants exhibited only white colonies. (B) ChIP analysis of the ectopic *cenH-ade6<sup>+</sup>* with Swi6 and H3 Lys<sup>9</sup>-methyl antibodies in wild-type (WT) and RNAi deletion strains. The primer pair amplifies different-sized fragments from the *cenH-ade6<sup>+</sup>* locus and the *ade6DN/N* minigene at the endogenous location.

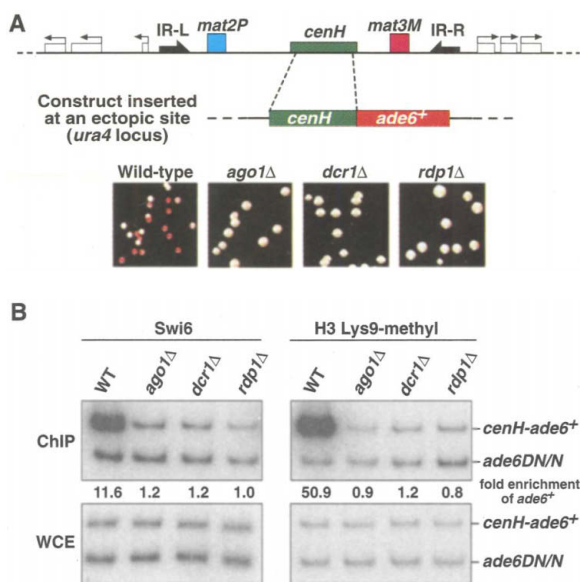
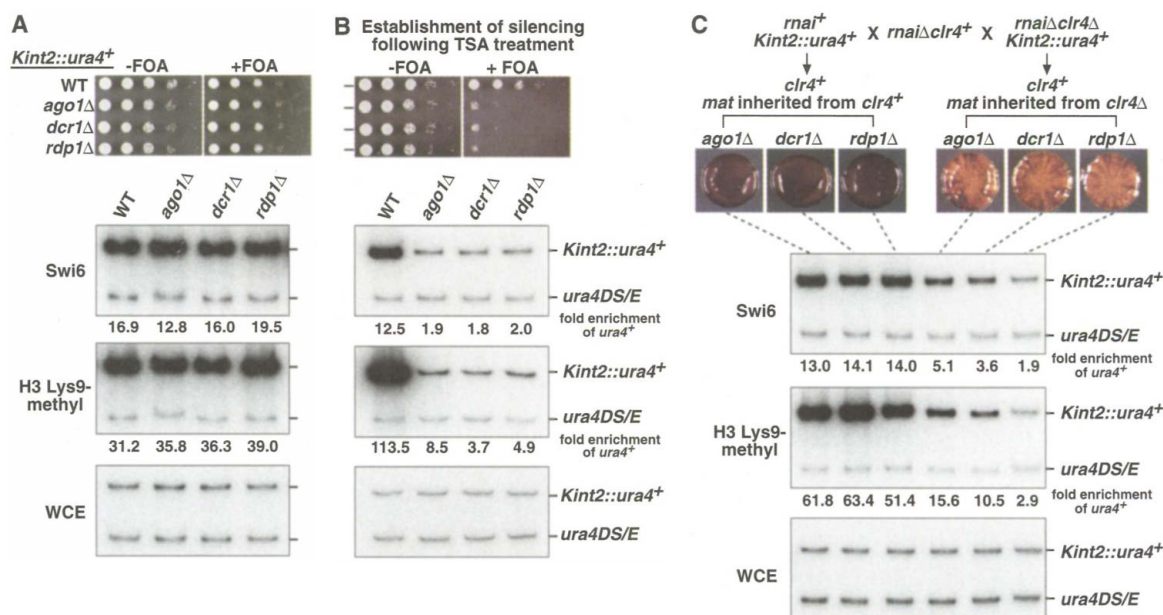


**Fig. 5.** The RNAi machinery is required for initiation of heterochromatin at the mating-type locus. (A) RNAi mutants are dispensable for the maintenance of heterochromatin at *Kint2::ura4<sup>+</sup>*. A heterochromatic *Kint2::ura4<sup>+</sup>* was introduced into the *ago1Δ*, *dcr1Δ*, and *rdp1Δ* mutant backgrounds by genetic crosses. Serial dilution plating assays (top) in the presence and absence of FOA were performed to measure *Kint2::ura4<sup>+</sup>* expression. Levels of Swi6 and H3 Lys<sup>9</sup> methylation at *Kint2::ura4<sup>+</sup>* in the strains were determined by ChIP analysis. (B) RNAi mutants are defective in the establishment of heterochromatin. Wild-type and mutant strains were treated with 35 μg of TSA per ml for 10 generations and were allowed to grow for an additional 10 generations in the absence of TSA. Expression of *Kint2::ura4<sup>+</sup>* is shown by serial dilution analysis (top). Levels of Swi6 and H3 Lys<sup>9</sup> methylation at *Kint2::ura4<sup>+</sup>* after recovery from TSA treatment were determined by ChIP. (C) RNAi mutants cannot efficiently initiate heterochromatin formation. A mating-type region derived from wild-type or *clr4Δ* background was introduced into the RNAi mutant backgrounds by genetic crosses (top). Diploids were constructed by



crossing the indicated strains, sporulated, and subjected to tetrad analysis. The *maiΔclr4<sup>+</sup> Kint2::ura4<sup>+</sup>* segregants from each cross were assayed for silencing and efficiency of mating-type switching, which also depends on heterochromatin assembly at the *mat* locus. To assay mating-type switching, colonies were replicated onto sporulation medium (PMA<sup>+</sup>) and stained with iodine vapors. Dark staining indicates efficient *mat* switching, and light or sector staining indicates defects in switching and heterochromatin formation. Levels of Swi6 and H3 Lys<sup>9</sup> methylation at the *mat* locus of the indicated cultures were assayed by ChIP.

References and Notes

- W. Reik, J. Walter, *Curr. Opin. Genet. Dev.* **8**, 154 (1998).
- S. I. S. Grewal, S. C. Elgin, *Curr. Opin. Genet. Dev.* **12**, 178 (2002).
- D. E. Cohen, J. T. Lee, *Curr. Opin. Genet. Dev.* **12**, 219 (2002).
- G. Cavalli, *Curr. Opin. Cell Biol.* **14**, 269 (2002).
- S. Henikoff, *Biochim. Biophys. Acta* **1470**, 1 (2000).
- B. D. Strahl, C. D. Allis, *Nature* **403**, 41 (2000).
- T. Jenuwein, C. D. Allis, *Science* **293**, 1074 (2001).
- J. A. Birchler, M. P. Bhadra, U. Bhadra, *Curr. Opin. Genet. Dev.* **10**, 211 (2000).
- J. Hsieh, A. Fire, *Annu. Rev. Genet.* **34**, 187 (2000).
- D. R. Dorer, S. Henikoff, *Cell* **77**, 993 (1994).
- Y. Chikashige et al., *Cell* **57**, 739 (1989).
- K. M. Hahnenberger, J. Carbon, L. Clarke, *Mol. Cell. Biol.* **11**, 2206 (1991).
- R. C. Allshire, E. R. Nimmo, K. Ekwall, J. P. Javerzat, G. Cranston, *Genes Dev.* **9**, 218 (1995).
- H. Nakagawa et al., *Genes Dev.* **16**, 1766 (2002).
- K. Ekwall, T. Ruusala, *Genetics* **136**, 53 (1994).

16. G. Thon, A. Cohen, A. J. Klar, *Genetics* **138**, 29 (1994).  
 17. S. I. S. Grewal, M. J. Bonaduce, A. J. Klar, *Genetics* **150**, 563 (1998).  
 18. J. Nakayama, J. C. Rice, B. D. Strahl, C. D. Allis, S. I. S. Grewal, *Science* **292**, 110 (2001).  
 19. K. Noma, C. D. Allis, S. I. S. Grewal, *Science* **293**, 1150 (2001).  
 20. S. I. S. Grewal, A. J. Klar, *Genetics* **146**, 1221 (1997).  
 21. J. Nakayama, A. J. Klar, S. I. S. Grewal, *Cell* **101**, 307 (2000).  
 22. S. I. S. Grewal, A. J. Klar, *Cell* **86**, 95 (1996).  
 23. K. Noma, S. I. S. Grewal, unpublished data.  
 24. N. Ayoub, I. Goldshmidt, R. Lyakhovetsky, A. Cohen, *Genetics* **156**, 983 (2000).  
 25. G. J. Hannon, *Nature* **418**, 244 (2002).  
 26. M. Wassenecker, *Plant Mol. Biol.* **43**, 203 (2000).  
 27. M. Matzke, A. J. M. Matzke, J. M. Kooter, *Science* **293**, 1080 (2001).  
 28. L. Aravind, H. Watanabe, D. J. Lipman, E. V. Koonin, *Proc. Natl. Acad. Sci. U.S.A.* **97**, 11319 (2000).  
 29. G. Hutvagner, P. D. Zamore, *Curr. Opin. Genet. Dev.* **12**, 225 (2002).  
 30. T. Volpe, C. Kidner, I. M. Hall, G. Teng, S. I. S. Grewal, R. A. Martienssen, *Science*, **297**, 1833 (2002).  
 31. B. J. Reinhart, D. P. Bartel, *Science*, **297**, 1831 (2002).  
 32. A. Akhtar, D. Zink, P. B. Becker, *Nature* **407**, 405 (2000).  
 33. A. J. Bannister *et al.*, *Nature* **410**, 120 (2001).  
 34. V. Jackson, R. Chalkley, *Biochemistry* **24**, 6930 (1985).  
 35. E. Heard *et al.*, *Cell* **107**, 727 (2001).  
 36. E. U. Selker, *Cell* **97**, 157 (1999).  
 37. M. Pal-Bhadra, U. Bhadra, J. A. Birchler, *Mol. Cell* **9**, 315 (2002).  
 38. We thank W. Tansley and J. Rice for critical reading of the manuscript; J. Nakayama, R. Martienssen, and G. Hannon for helpful contributions; D. Bartel for sharing unpublished results; and G. Xiao and Y. Tsukamoto for technical assistance. I.M.H. is an Arnold and Mabel Beckman Fellow and thanks S. Nuñez for her support. Funded by grants from Ellison Medical Foundation and the National Institutes of Health (GM59772) to S.I.S.G. and the Israel Science Foundation (N157/00-1) to A.C.

22 July 2001; accepted 14 August 2002

Published online 5 September 2002;

10.1126/science.1076466

Include this information when citing this paper.

## REPORTS

## Orbital Ordering Transition in $\text{La}_4\text{Ru}_2\text{O}_{10}$

P. Khalifah,<sup>1,2\*</sup> R. Osborn,<sup>3</sup> Q. Huang,<sup>4,5</sup> H. W. Zandbergen,<sup>2,6</sup> R. Jin,<sup>7†</sup> Y. Liu,<sup>7</sup> D. Mandrus,<sup>8</sup> R. J. Cava<sup>1,2</sup>

We report experimental evidence for a full orbital ordering transition in the two-dimensional lanthanum ruthenate  $\text{La}_4\text{Ru}_2\text{O}_{10}$ . The observable consequences of this orbital ordering include the loss of the Ru local moment, a structural distortion which partitions Ru-O bonds into axially oriented short and long sets, a sharp jump in electrical resistivity, and the opening of a spin gap that is visible in neutron scattering experiments. This is a rare example of a discrete orbital ordering transition in a 4d transition metal oxide and demonstrates that orbital effects can have an influence on the properties of layered ruthenates, a family of compounds that notably includes the p-wave superconductor  $\text{Sr}_2\text{RuO}_4$  and the field-tuned quantum critical metamagnet  $\text{Sr}_3\text{Ru}_2\text{O}_7$ .

The study of the interplay between orbital, spin, and charge degrees of freedom in transition metal oxides is at the forefront of condensed-matter physics (1). Invariably, the canonical examples of orbitally ordered compounds [including  $\text{YTiO}_3$  (2),  $\text{YVO}_3$  (3),

$\text{KCuF}_3$  (4), and the perovskite manganites (5–8)] contain 3d transition metals because they display large magnetic moments and strong coupling of orbital and charge configurations to local coordination polyhedron geometry. Recently, evidence has been mounting for the importance of orbital physics in perovskite-related structures containing the 4d transition metal ruthenium (Ru). Inelastic x-ray scattering experiments have found evidence for partial orbital ordering in the compound  $\text{Ca}_2\text{RuO}_4$  (9), and theoretical models for treating the orbital effects in this system have been developed (10, 11). Unfortunately, it is difficult to assess the effects of orbital ordering on the properties of  $\text{Ca}_2\text{RuO}_4$ , because the ordering is estimated to be only 50% complete [the  $d_{xy}$  orbital occupancy is augmented from 50 to 75% on cooling from 300 K to 90 K] (9), and the shift of orbital population gradually occurs over a tempera-

ture.

